Full Paper

Propellants, Explosives, Pyrotechnics

DOI: 10.1002/prep.201400017

# Burning Characteristics of Microcellular Combustible Objects Fabricated by a Confined Foaming Process

**Weitao Yang,[a] Yuxiang Li,[a] and Sanjiu Ying*[a]**

**Abstract**: Microcellular combustible objects for application of combustible case ammunition and caseless ammunition were fabricated by a confined pressure quenching foaming process using supercritical $CO_2$ as foaming agent. The experimental results showed that the force constant (*f*) of objects obviously increased with an increasing RDX content and that the force constant of formulation with 55% RDX is comparable to that of traditional felted case. Pressure histories, *dp*/*dt*-*t*, and dynamic vivacity curves were investigated and compared by closed vessel tests. The influencing factors such as RDX content, expansion ratio, foaming temperature, sample size, and loading density were analysed. The results revealed that RDX content and expansion ratio significantly affected the burning properties, whereas the foaming temperature did not have obvious influence. Moreover, the burning behavior also changed with sample size and loading density.

**Keywords:** Microcellular combustible objects · Burning characteristics · Closed vessel test · Confined foaming process · Supercritical $CO_2$

## 1 Introduction

The use of porous combustible objects in application of combustible cartridge cases ammunition [1–4] or caseless ammunition [5–7] for weapons offers a number of advantages. First, the elimination of metallic case brings with a sizeable weight reduction. Second, the burden of disposing of spent metal case is relieved. Third, automatic firing devices can be consequently applied. Fourth, combustible cartridge case adds energy to propel a projectile. In general, porous structure is required for complete consumption and high burning rate when the objects burn in gun. Therefore, various methods have been proposed and investigated [1,8,9], such as felt-moulding, winding, and impregnation of resin in the felted combustible components. Due to the absence of a protective metallic case, there are very strict requirements regarding the material properties of porous objects. Combustible cases with high energy content, good heat resistance and low sensitivity of the material properties are needed. Nevertheless, traditional formulations using nitrocellulose (NC) as energetic ingredient are judged to be unsafe due to an increased sensitivity to outer stimulations [10]. Propellants based on polymer bonded nitramines are distinguished from NC-based propellants by low vulnerability [11, 12]. In recent years, reaction injection moulding (RIM) processes [5,6] have been employed to produce RDX-based foamed propellants.

Because the combustible objects contain large amounts of pores, it is believed that a convective combustion zone ahead of the flame front, resulting from the infiltration of combustion products through pores, is responsible for the in-depth combustion or volumetric combustion phenomena [10]. But, combustible objects, which exhibit such a wide range of chemical composition and inner structure might not be expected to burn following a single combustion mechanism. Indeed, differences in the binder material, factors related to the oxidizer (RDX, HMX, or TAGN), and factors related to porous structure (porosity, pore size or pore size distribution) influence the burning behaviors.

In our previous work, RDX-based microcellular combustible objects were fabricated by confined foaming process using supercritical $CO_2$ (SC-$CO_2$) and influencing factors, which affected inner structure were also discussed [13]. Figure 1 presents a typical inner structure of the object. For laboratory experimentation, an important diagnostic involves the use of a closed vessel, in which the pressure history of a burning propellant is recorded. From the pressure history, information concerning the combustion of the objects can be deduced and used in ballistic simulations to estimate potential performance. In this paper, the combustion behaviors and influencing factors were investigated.

## 2 Experiments Section

### 2.1 Materials and Sample Preparing

The combustible objects based on inert binder poly methyl methacrylate (PMMA, Altuglas® V 040) and RDX (10 μm)

[a] *W. Yang, Y. Li, S. Ying*
*School of Chemical Engineering*
*Nanjing University of Science and Technology*
*Nanjing, 210094. P. R. China*
**e-mail: yingsanjiu@126.com*

  

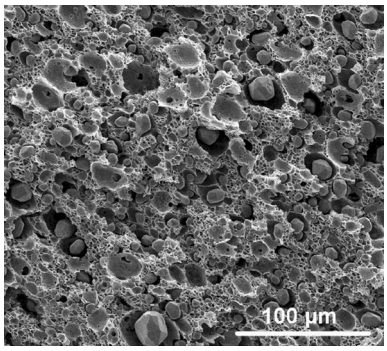


**Figure 1.** Inner structure of foamed sample (RDX content = 60 %, foaming temperature = 60 °C, saturation pressure = 15 MPa, decompression time = 30 s).

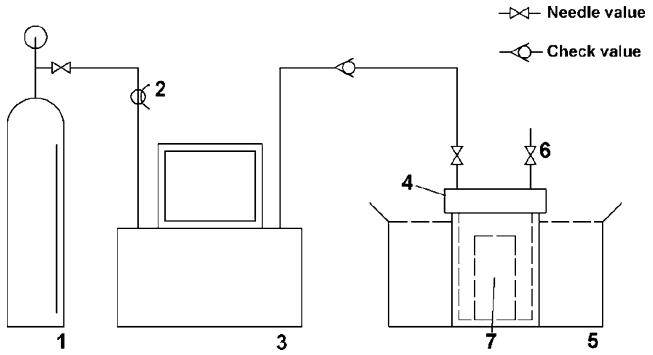


**Figure 2.** Self-developed device for supercritical carbon dioxide foaming: 1. $CO_2$ cylinders, 2. Cooling circulation system, 3. Booster pump and Control system, 4. High pressure vessel, 5. Thermostatic waterbath, 6. Vent valve, 7. Foaming mould.

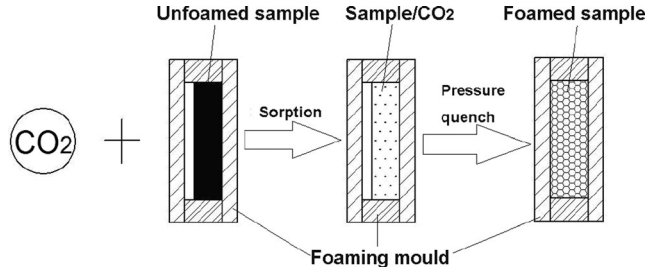


**Figure 3.** Schematic diagram of confined foaming process.

were formulated. The object formulations were processed on the laboratory scale (200 g batch) by solvent procedures. All components were filled in a sigma blade mixer to obtain homogeneous dough. The dough was subsequently extruded to form preforms in a vertical hydraulic press of 630 KN capacity. The extruded preforms were dried in a water bath oven at 30 °C for 24 h, 40 °C for 24 h and 50 °C till the volatile matter was brought to the level of $<0.5$ percent. Afterwards, the preforms were cut to $50\times 12.9\times 2.0$ mm.

Figure 2 and Figure 3 present the self-developed device and confined foaming process, respectively. All foaming experiments were performed in a high pressure vessel, with a capacity of about 270 $cm^3$, operating at different temperatures and a constant pressure of 15 MPa. The temperature was controlled by thermostatic waterbath. The vessel was built in gun steel, with a cylindrical vessel of 4.5 cm diameter and 27 cm of depth. Sheet preforms were foamed in moulds, as described previously [11].

**Table 1.** Sample densities [$g\,cm^{-3}$].

| RDX content [wt-%] | Expansion ratio ($\phi$) | | | |
|---|---|---|---|---|
| | 1.0 [a] | 1.1 | 1.2 | 1.35 |
| 60 | 1.49 | 1.35 | 1.24 | 1.10 |
| 65 | 1.55 | 1.41 | 1.29 | 1.15 |
| 70 | 1.61 | 1.46 | 1.34 | 1.19 |
| 75 | 1.67 | 1.52 | 1.39 | 1.24 |

a) Refers to unfoamed sample.

The densities of unfoamed samples with different RDX contents were measured using Xu's [14] method and the densities of samples with different expansion ratios ($\phi$) could be obtained (Table 1).

### 2.2 Burning Characteristics Analysis

The burning characteristics were studied by statically evaluating the samples at 0.12 and 0.20 loading densities ($\Delta$) in 109 mL closed vessel. All samples were fired by 2 # nitrocellulose under the same ignition pressure (10.98 MPa) at ambient temperature. The pressure histories were subsequently recorded.

Force constant ($f$) and gas covolume ($\alpha$) were calculated using the following equations set (GJB 5472. 9-2005):

$$\begin{cases} f = p_m / \Delta - \alpha \cdot p_m \\ \alpha = \left(p_{m2} / \Delta_2 - p_{m1} / \Delta_1\right) / \left(p_{m2} - p_{m1}\right) \end{cases}$$

The $dp/dt$-$t$ curves were reduced from the pressure histories and the dynamic vivacity ($L$) was calculated by the following formula:

$$L = \frac{1}{p\ p_m} \frac{dp}{dt}$$

## 3 Results and Discussions

The force constant ($f$) and gas covolume ($\alpha$) were calculated using maximum pressure at loading densities of 0.12 and 0.20, and the results are given in Figure 4. With increasing of RDX content, the force constant increased from 450.2 to 858.7 $J\,g^{-1}$ with a corresponding decrease in gas covolume from 1.61 to 1.05 $cm^3\,g^{-1}$. Figure 4 illustrates that the force constant of formulations with 55 % RDX is comparable to that of traditional felted combustible case (62 % nitrocellulose, 24.5 % kraft fibers and 13.5 % adhesive and addition agent) [15].

  

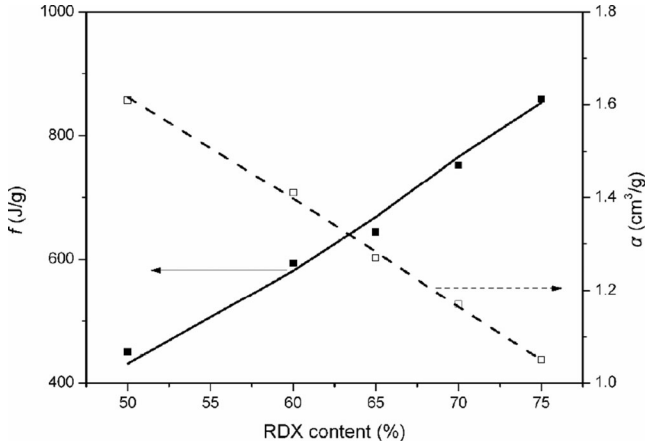


**Figure 4.** *f* and $\alpha$ of samples with various RDX contents.

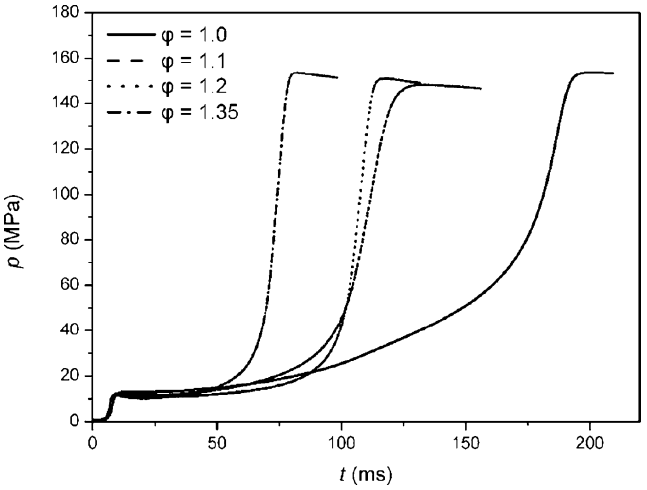


**Figure 5.** *p-t* curves for samples with various expansion ratios.

Usually, burning behaviors of porous combustible objects are not only determined by components and additives, but also by porosity and inner surface. Increased energetic filler favors decomposition and combustion of formulations. In the confined foaming process, the porosity is restricted by molds with varying expansion ratio. Increased expansion ratio can be interpreted as increased porosity, which favors gas penetration and convective burning. Moreover, the porous structure (pore size distribution) can also be adjusted effectively by changing foaming temperature. In addition, object size and loading density may also affect the combustion behaviors. The influencing factors will be discussed below.

### 3.1 Influence of Expansion Ratio

Samples with 60% RDX were foamed at 60 °C with different expansion ratios. The pressure histories are shown in Figure 5. As Figure 5 indicates, samples with decreased densities burned faster. Meanwhile, the pressure histories consist of combustion of the ignition powder, a subsequent slight pressure decrease due to heat transfer loss, and, finally, the combustion of microcellular sample.

Figure 6 shows the *dp*/*dt*-*t* curves. The curves all exhibit double peaks, i.e. the ignition powder combustion peak and the sample combustion peak. The ignition delay (*dp*/*dt* = 0) for each sample can be determined from the time between these two peaks. It was observed that as the expansion ratio increased, the time interval between the peaks decreased and the peak value increased. The sample with the highest expansion ratio was shown to have the shortest ignition delay. This is the result of both the increased conductivity coefficient and decreased density of the material [16]. The ignition delay performance is highly advantageous from heat resistance point of view.

Figure 7 shows the dynamic vivacity of samples with various expansion ratios. For the foamed samples, $p/p_m$ at the dynamic vivacity peak increased slightly in the range of 0.4

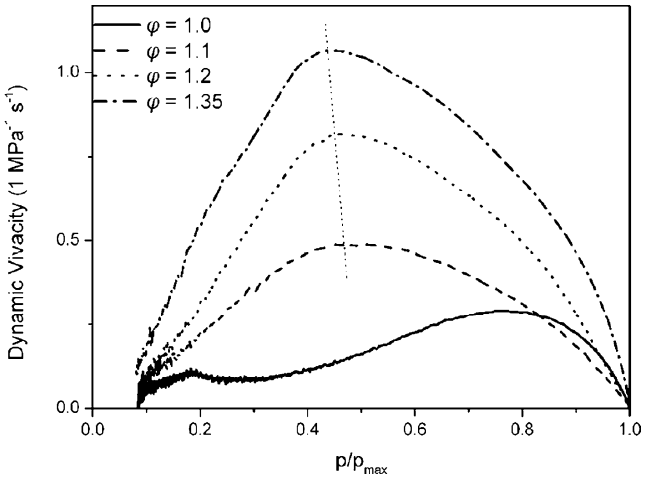


**Figure 6.** *dp*/*dt* curves of foamed samples with various expansion ratios.

to 0.5 with decreased expansion ratio, whereas the vivacity peak of unfoamed sample was obtained at $p/p_m = 0.8$, indicating a better progressivity. The difference between foamed and unfoamed samples indicates that different combustion modes were followed when foamed and unfoamed samples burned in closed vessel.

### 3.2 Influence of RDX Content

Keeping the expansion ratio (1.2) and foaming temperature (60 °C) constant, RDX content can influence the burning characteristics in a positive way. Figure 8 and Figure 9 show the *p-t* curves and *dp*/*dt* curves, respectively. As expected, when all was equal, formulations (either porous or nonporous) containing more energetic fillers tended to burn significantly faster and the maximum pressure were much higher. Meanwhile, as shown in Figure 9, as the RDX content increased, the time interval between the *dp*/*dt* peaks

  

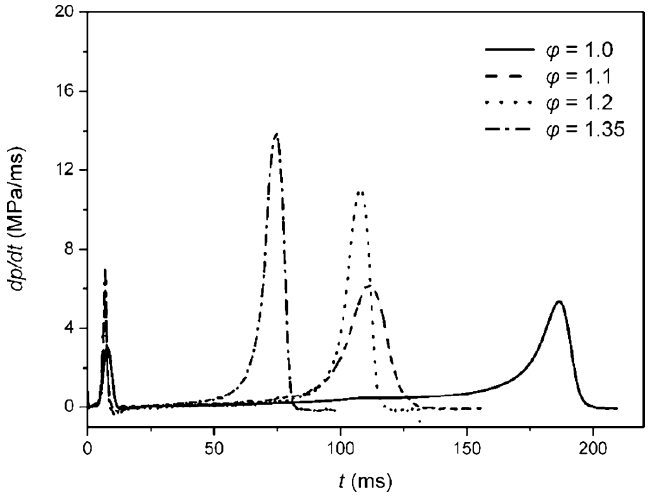


**Figure 7.** Dynamic vivacity of samples with various expansion ratios.

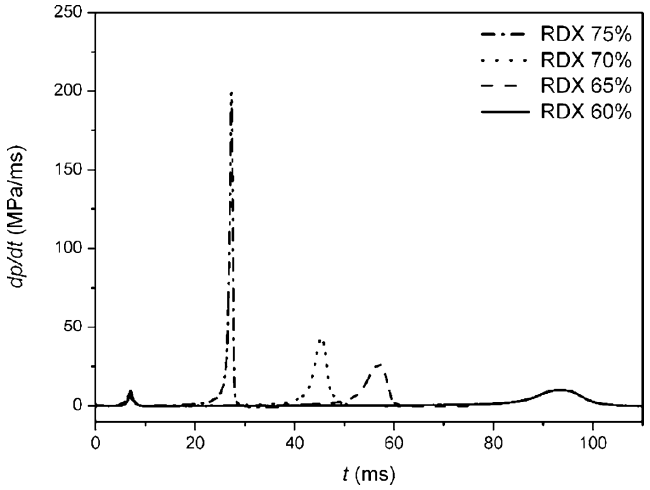


**Figure 9.** *dp*/*d*t curves of foamed samples with various RDX contents.

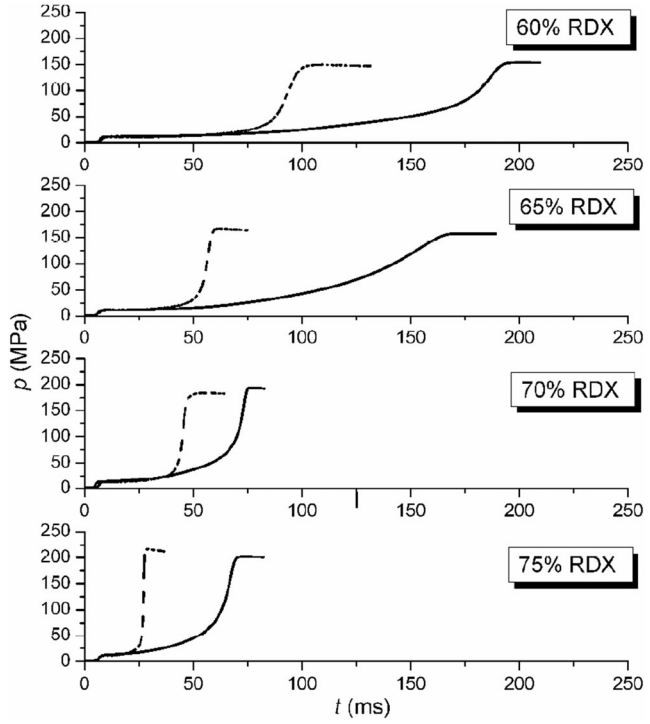


**Figure 8.** *p*-*t* curves of unfoamed and foamed samples with various RDX contents (full lines refer to unfoamed samples; broken lines refer to foamed samples).

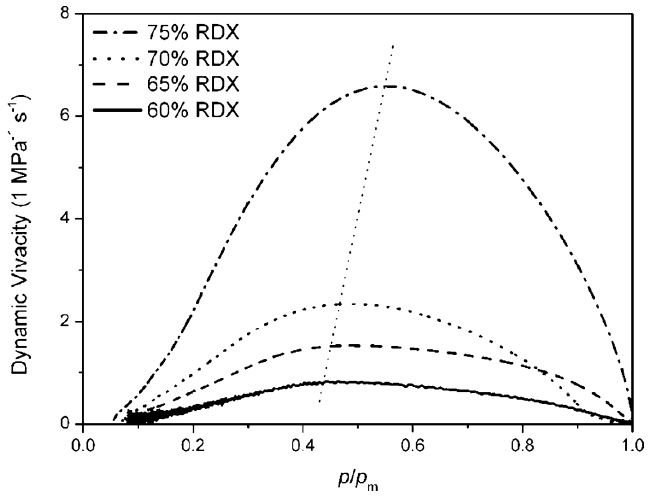


**Figure 10.** Dynamic vivacity of foamed samples as a function of RDX contents.

decreased and the peak value increased. The sample with the highest RDX content had the shortest ignition delay time.

Besides, the vivacity was also influenced by the content of the energetic component in an advantageous manner (Figure 10). With the increased RDX content in the formulation, the maximum dynamic vivacity increased from 0.83 to 6.58 $MPa^{-1}s^{-1}$ with a corresponding increase of *p*/*pm* values at maximum dynamic from about 0.45 to 0.6.

### 3.3 Influence of Foaming Temperature

Preforms with 60% RDX were foamed at 40 °C, 50 °C and 60 °C with expansion ratio of 1.2 to investigate the influence of foaming temperature on burning behaviors of foamed samples. The *p*-*t*, *dp*/*dt* curves and dynamic vivacities are displayed in Figure 11, Figure 12, and Figure 13.

As the three figures show, foaming temperature has no obvious influence on burning behaviors of samples once the expansion ratio is kept constant. Sample foamed at 50 °C burned fastest and sample foamed at 40 °C took a little longer time to burn out. As Figure 13 indicates, only insignificant variations can be observed and dynamic vivacity curves are very close to each other with *p*/*pm* = 0.45 at the vivacity peak.

  

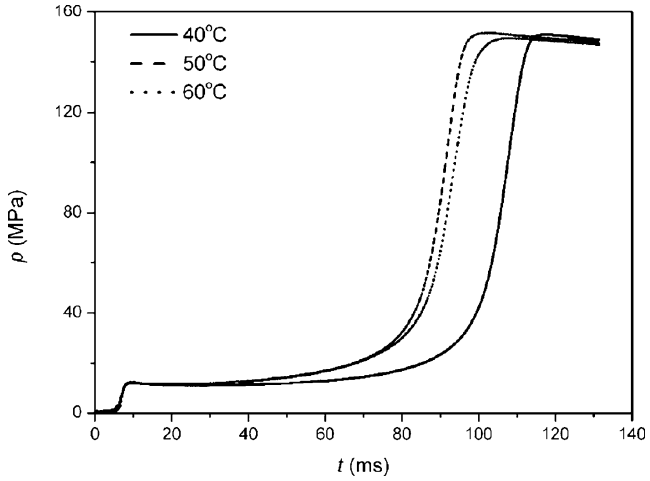


**Figure 11.** *p-t* curves of samples foamed at various temperatures.

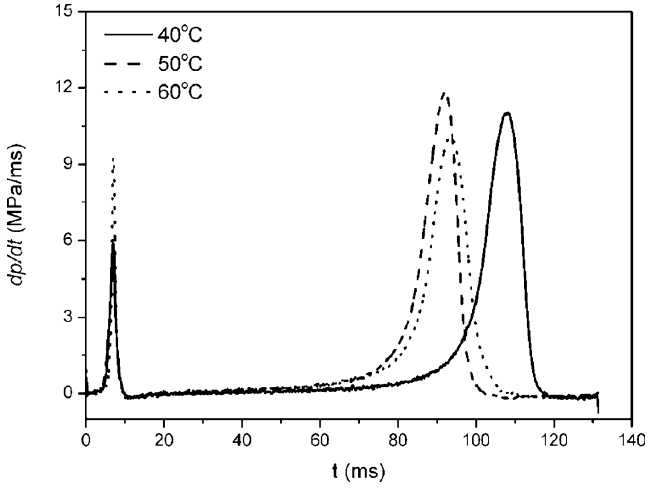


**Figure 12.** *dp/dt* curves of samples foamed at different temperatures.

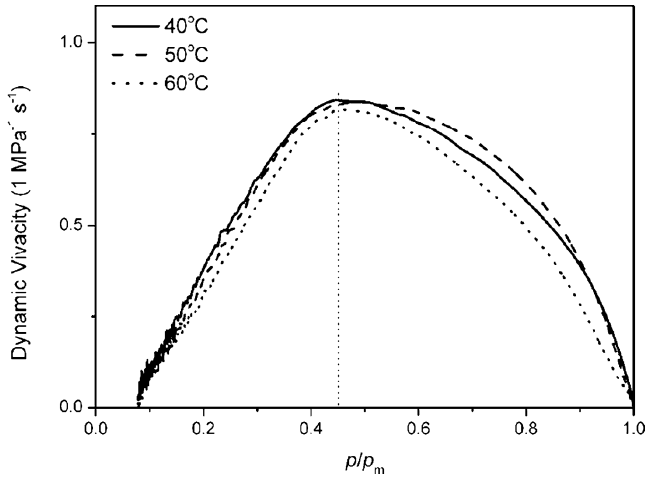


**Figure 13.** Dynamic vivacity of samples foamed at various temperatures.

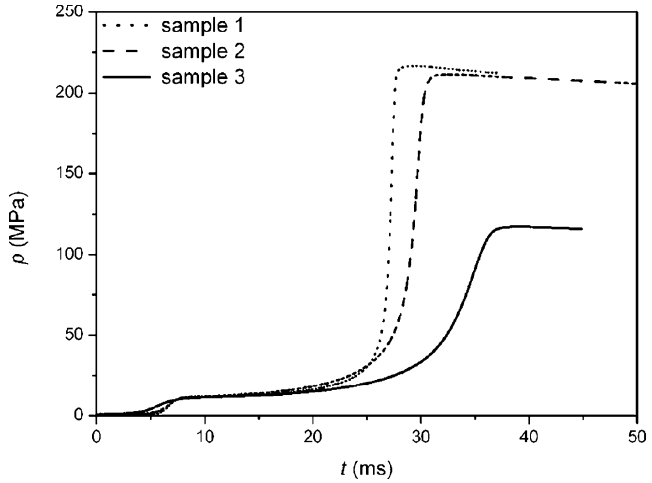


**Figure 14.** *p-t* curves of samples (75% RDX, $\phi = 1.2$, temperature = 60 °C).

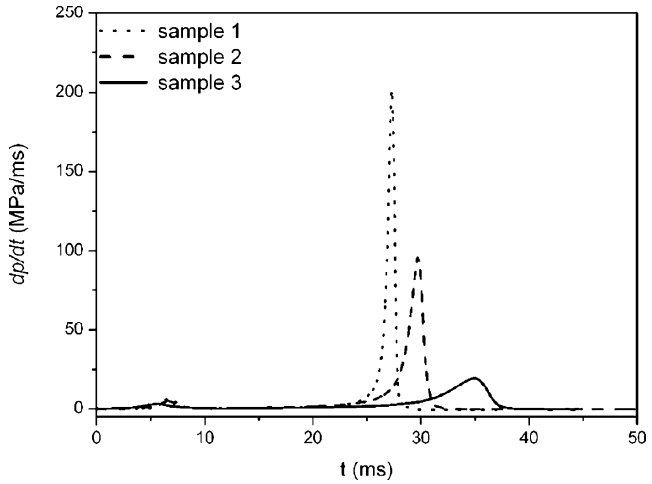


**Figure 15.** *dp/dt* curves of samples (75% RDX, $\phi = 1.2$, temperature = 60 °C).

### 3.4 Dependence of Burning Behaviors on Sample Size and Loading Density

The differences in burning rate associated with sample size and loading density were observed when other porous combustible materials were tested [17, 18]. Hence, three samples were prepared to investigate the influence of sample size and loading density on burning behaviors. All samples were foamed at the same conditions with constant expansion ratio. Thickness of sample 1 and sample 3 is 2.4 mm, and thickness of sample 2 is 4.8 mm, respectively. Sample 1 and 2 were tested at loading density of 0.20, and sample 3 was conducted under $\Delta = 0.12$. The results of closed vessel test are listed in Figure 14, Figure 15, and Figure 16.

Comparing sample 1 with 2, thin sample burned faster than thick one and the ignition delay of the two samples

  

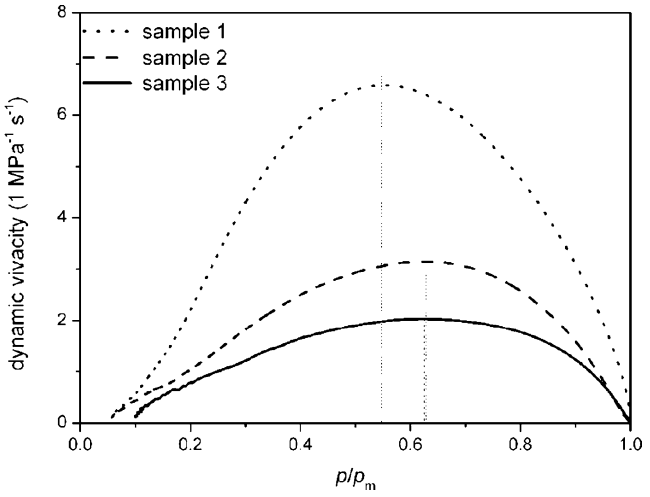


**Figure 16.** Dynamic vivacity of samples (75% RDX, $\phi = 1.2$, temperature = 60 °C).

were almost identical. A significant difference in the values of maximum *dp/dt* for samples with different thickness can also be observed in Figure 15. Traditionally, gun/artillery propellants were extruded into progressive geometry such as 7- or multi-perforated shape to improve ballistic efficiency [19]. Dynamic tracks in Figure 16 indicate that sheet foamed samples burned progressively as the propellants with progressivity configuration.

## 4 Conclusions

This paper studied the burning characteristics of microcellular combustible objects and the influencing factors. Burning characteristics of foamed propellants can be adjusted by the variation of the energetic ingredients and expansion ratio. Meanwhile, combustion behaviors are also affected by shape of ammunition and loading density. Due to these manifold possibilities to adjust the specific performance, microcellular combustible objects can be adapted and fine tuned for a variety of applications. Since the relative density ($1/\phi$) of the objects and the ratio of energetic fillers can influence the burning characteristics in an opposite manner, burning rate and specific energy can be adjusted independently from each other. Analysis and form function techniques more complex than the laminar burning, uniform densities are necessary to model the burning mechanism of the objects.

## *Acknowledgments*

This project is funded by the Priority Academic Program Development of Jiangsu Higher Education Institutions.

## References

[1] P. L. Deluca, J. C. Williams, Fibrillated Polyacrylic Fiber in Combustible Cartridge Cases, *Ind. Eng. Chem. Prod. Res. Dev.* **1984**, *23*, 438 – 441.
[2] M. T. Shedge, C. H. Patel, S. K. Tadkod, G. D. Murthy, Polyvinyl Acetate Resin as a Binder Effecting Mechanical and Combustion Properties of Combustible Cartridge Case Formulations, *Def. Sci. J.* **2008**, *58*, 390 – 397.
[3] G. R. Kurulkar, R. K. Syal, H. Singh, Combustible Cartridge Case Formulation and Evaluation, *J. Energ. Mater.* **1996**, *14*, 127 – 149.
[4] F. Zimmerman, Development of 7.62-mm and 38-mm Combustible Cartridge Case Ammunition, *J. Spacecr. Rockets* **1969**, *6*, 312–314.
[5] J. Böhnlein-Mauß, H. Kröber, Technology of Foamed Propellants, *Propellants Explos. Pyrotech.* **2009**, *34*, 239 – 244.
[6] J. Böhnlein-Mauß, A. Eberhardt, T. S. Fischer, Foamed Propellants, *Propellants Explos. Pyrotech.* **2002**, *27*, 156 – 160.
[7] R. M. Price, R. Reed Jr., *Thermally Stable Gun and Caseless Cartridge Propellants*, US Patent 4,263,070, Thiokol Corporation, Newtown, PA, USA, **1981**.
[8] R. I. Brabets, *Combustible Cartridge Case Characterization*, US Govt Report AD-A140 664, **1984**.
[9] K. O. Jacobsen, E. Troen, *Combustible Cartridge Casings and Method for Making Same*, US Patent 3,977,325, A/S Raufoss Ammunisjonsfabrikker, Norway, **1976**.
[10] J. T. Barnes, E. B. Fisher, *Combustion Mechanism of Very High Burn Rate (VHBR) Propellant*, Army Research Laboratory, Report No. ARECR-242, Washington, DC, USA, **1995**.
[11] R. R. Sanghavi, P. J. Kamale, M. A. R. Shaikh, S. D. Shelar, K. S. Kumar, A. Singh, HMX-Based Enhanced Energy LOVA Gun Propellant, *J. Hazard. Mater.* **2007**, *143*, 532–534.
[12] A. G. S. Pillai, R. R. Sanghavi, C. R. Dayanandan, M. M. Joshi, S. P. Velapure, A. Singh, Studies on RDX Particle Size in LOVA Gun Propellant Formulations, *Propellants Explos. Pyrotech.* **2001**, *26*, 226–228.
[13] W. Yang, Y. Li, S. Ying, Fabrication, Thermoanalysis, and Performance Evaluation Studies on RDX-Based Microcellular Combustible Objects, *Propellants Explos. Pyrotech.* **2014**, accepted, DOI:10.1002/prep.201400022.
[14] Q. Xu, X. Ren, Y. Chang, J. Wang, L. Yu, K. Dean, Generation of Microcellular Biodegradable Polycaprolactone Foams in Supercritical Carbon Dioxide, *J. Appl. Polym. Sci.* **2004**, *94*, 593 – 597.
[15] Y. Li, D. Guo, C. W. Zhao, W. L. Zhou, F. M. Xu, Characterization of Combustible Cartridge Cases Enhanced by Novel Energetic Fibers, *Chin. J. Energ. Mater.* **2009**, *3*, 023.
[16] A. K. Kulkarni, M. Kumar, K. K. Kuo, Review of Solid-Propellant Ignition Studies, *AIAA J.* **1982**, *20*, 243 – 244.
[17] J. W. Colburn, F. W. Robbins, *Combustible Cartridge Case Ballistic Characterization* (*No. BRL-MR-3835)*. Army Ballistic Research Lab Aberdeen Proving Ground, MD, USA, **1990**.
[18] T. S. Fischer, A. Messmer, Burning Characteristics of Foamed Polymer-Bonded Propellants, *19th International Symposium of Ballistics*, *Interlaken*, Switzerland, 7–11 May **2001**, pp. 107–114.
[19] D. Mueller, New Gun Propellant with CL-20, *Propellants Explos. Pyrotech.* **1999**, *24*, 176–181.

Received: January 16, 2014
Revised: April 15, 2014
Published online: May 26, 2014

  